Deep-Sea Research, Vol. 37, No. 6, pp. 1053–1074, 1990.
Printed in Great Britain.

0198–0149/90 $3.00 + 0.00

Baroclinic instabilities and forced oscillations in the Brazil/Malvinas confluence front

SILVIA GARZOLI* and CLAUDIA SIMIONATO†

(*Received* 20 *March* 1989; *in revised form* 1 *February* 1990; *accepted* 20 *February* 1990)

Abstract—Observations collected at the confluence between the Brazil and Malvinas currents are analysed to study the high-frequency oscillations in the range of periods from 55 to 2 days. The variability in time and space of the thermohaline front originates at the confluence. The meandering of the Brazil Current after the encounter and the presence of an abrupt shelf break, create the conditions for the generation of baroclinic and internal waves. Analysis of time-series of dynamic height, wind magnitude, and position of the front indicates the following: in the band from 20 to 55 day periods, two waves propagate with similar characteristics but in the opposite direction; neither of these waves appears to be forced by the wind. The westward-propagating wave ($T = 37.4$ days) is related to the position of the front and is assumed to be forced by its north–south displacement. The eastward-propagating wave ($T = 29.1$ days) has the characteristics of a topographic Rossby wave. At shorter periods, in the band from 2 to 10 days, the spectrum of the atomosphere is very energetic. The passage of cyclones can be detected by the seasonal variability of the energy spectra. The ocean is forced by the wind at periods of 5 and 2.6 days. In addition to these wind-forced oscillations, the presence of the front originates baroclinic instabilities in the same band.

INTRODUCTION

DURING the past several years, an intensive program was carried out in the southwestern Atlantic to study the dynamics and water mass characteristics of the area in which the warm saltier water of the Brazil Current meets the cold fresher water from Malvinas. This area, that is referred to as the confluence region, contains complicated and interesting dynamics. The encounter of the two currents occurs around 38°S and creates a strong thermal front; the position of the confluence front varies in time and space due to the variability of the latitude of separation of the Brazil Current (OLSON *et al.*, 1988; GARZOLI and GARRAFFO, 1989). After the encounter, the Brazil Current turns northeastwards following a meandering path (RODEN, 1986); warm and cold eddies are ejected from the main flow (LEGECKIS and GORDON, 1982; GORDON, 1989). The available potential energy of these eddies is estimated to be of the same order of magnitude as the Gulf Stream rings (GARZOLI and GARRAFFO, 1989). A recent description of the characteristics of the region derived from the analysis of the collected data is given by OLSON *et al.* (1988).

This program consisted of extensive hydrographic surveys, analysis of satellite infra-red

*Lamont-Doherty Geological Observatory of Columbia University, Palisades, NY 10964, U.S.A.
†Centro para la Investigacion de la Dinamica del Mar y la Atmosfera, CIMA/CONICET, Tacuari 1183, 1071 Buenos Aires, Argentina.

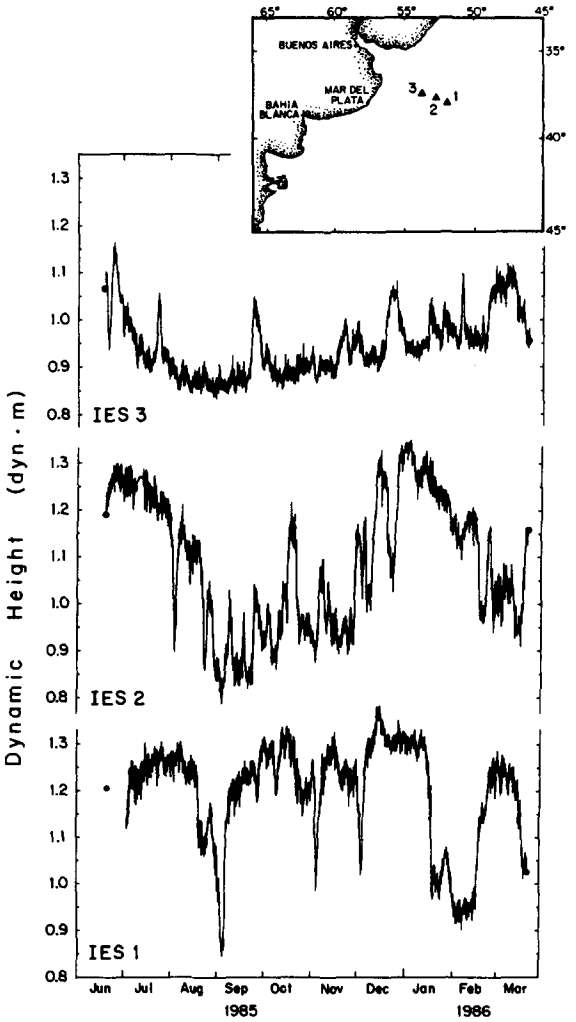

Fig. 1. Location of the deployments and hourly sampled series of dynamic height (surface relative to 800 m) for the period June 1985 to March 1986. ⊗ indicates dynamic height values calculated from hydrographic data.

images, launching of surface drifters and deployment of inverted echo sounders. Inverted echo sounders (IES) were deployed as a small array of three instruments in the frontal region. Time-series of travel time and ambient noise level were obtained at the three locations (Fig. 1). From the travel time-series, dynamic height and distance from the instruments to the front were obtained (GARZOLI and BIANCHI, 1987). The ambient noise level was correlated to the intensity of the wind stress at the surface (GARZOLI and CLEMENTS, 1986). The complete set of data was analysed by GARZOLI and GARRAFFO (1989). The low-frequency variability (seasonal and annual) of the time-series related to the frontal motion was studied and an estimate of geostrophic velocities associated with the main flows was obtained. The main conclusion of this previous work is that the dominant motion of the front is a low-frequency east–west displacement with a period

close to one year and related to the variability in the latitude of separation of the Brazil Current.

In addition to the low-frequency signal, the sounders' records are rich in high-frequency oscillations in the range from 0.025 to 0.020 cpd (40–55 days, the lowest resolved in this study) to tidal frequencies. This is not surprising since eddies, meanders and instabilities of the front dominate the dynamics. Similar oscillations were observed in frontal zones (MYSAK and SCHOTT, 1977; BRYDEN and PILLSBURY, 1977; BAKER *et al.*, 1977) and in the Gulf Stream (HOGG, 1981; JOHNS and WATTS, 1985, 1986; LUYTEN, 1977). In the Gulf Stream energetics in these periods have been detected. Topographic Rossby waves, characterized by an eastward phase propagation (OU and BEARDSLEY, 1980) and with periods greater than 8 days (THOMPSON and LUYTEN, 1976) have been reported shoreward of the Gulf Stream by several authors (THOMPSON, 1977; JOHNS and WATTS, 1985, 1986; HOGG, 1981). The possible mechanism of generation has been suggested to be the forcing of the large meanders (HOGG, submitted) and the rings shed by the main flow (LOUIS and SMITH, 1982). Meander-associated motions, many of them related to baroclinic instabilities of the Gulf Stream, have been observed in the whole band from 2 to 30 days (WEBSTER, 1961; BROOKS and BANE, 1981; WATTS and JOHNS, 1982; JOHNS and WATTS, 1985, 1986), though they have been shown to be dominant for periods shorter than 12–14 days (JOHNS and WATTS, 1985, 1986).

In this paper, simultaneous records of dynamic height and ambient noise level in the water column (a quantity proportional to the magnitude of the wind stress at the surface) will be analysed through statistical methods to study the dominant oscillations in the records. The characteristics of these oscillations will be analysed in an effort to establish their origin and forcing mechanisms.

OBSERVATIONS

In two consecutive experiments, inverted echo sounders (IES) were deployed in the southwestern Atlantic (Argentine Basin) for periods of approximately 8 months (two instruments) and 9 months (three instruments). The sample period during the whole experiment was November 1984 to April 1986. In addition to the standard detection of travel time, the IES were equipped with an ambient noise capability to measure the magnitude of the wind stress at the surface.

Travel time and ambient noise level data obtained with the instruments were scaled to dynamic height relative to 800 m and to magnitude of the wind speed, respectively. A description of the instruments, an explanation and justification of the methods and a discussion on the errors incurred using the procedures for the calibration to dynamic height are given by GARZOLI and BIANCHI (1987) and GARZOLI and GARRAFFO (1989). Due to a malfunction of the instrument during the first part of the experiment, the time sampling period for the IES 3 was reduced to a block average of 2 days. Therefore only one 17-month long time-series of dynamic height and magnitude of the wind speed with 1 h resolution at IES 1 was obtained for the entire experiment. Three simultaneous 9-month time-series covering the second part of the experiment are available with a sampling period of 1 h. In this paper the analysis is based mainly on the analysis of the three 9-month simultaneous time-series and on the complete hourly sampled 17-month series obtained at the easternmost location, IES 1. The location of the instruments whose data is to be analysed in this paper, the depth of the deployments, and the sampling period are given in

Table 1. Location and depth of the deployments, period covered by the observations analysed in this paper and sampling period

Station	Latitude	Longitude	Depth (m)	First/last sample	Δt (h)
IES 3	37°28.91'S	53°49.39'W	1112	06/18/85–03/23/86	1
IES 2	37°46.46'S	52°45.52'W	3803	06/19/85–03/23/86	1
IES 1	37°58.70'S	51°56.40'W	4351	11/09/84–06/20/85	1/2
IES 1	37°58.08'S	51°56.37'W	4350	06/20/85–03/24/86	1

Table 1. The time-series of dynamic height relative to 800 m obtained at the three locations during the second part of the experiment are shown in Fig. 1.

It has been shown that it is possible to obtain a measurement of the wind speed from the bottom of the ocean (i.e. LEMON *et al.*, 1984). This can be done by sensing the ambient noise in the water column to which, at frequencies above 2 kHz, the surface wind is the main contributor (KNUDSEN *et al.*, 1948). The procedure to obtain wind magnitude from the ambient noise records is explained by GARZOLI and CLEMENTS (1986). In general, there is a good correlation between the noise in the water column and the pressure that the wind stress exerts at the surface. The error of the estimate is $\pm$ 1.5 m s^{-1}. For the second set of observations, new wind data obtained during the deployment and recovery cruises allowed us to improve the calibration of the ambient noise records at the IES 1 and IES 3 locations, but no set of *in situ* wind data was obtained at IES 2. In order to make data from IES 2 usable for this analysis, it was decided that the calibration of this last unit could be done using the values of the wind obtained at IES 1. IES 1 is located 100 km from IES 2 and deployed at approximately the same depth. Data were adjusted to maintain the same level of energy at very low frequencies. It can be shown that the low-frequency magnitude of the wind is the same at both locations by analysing the spatial scale that in the area is larger than 100 km. With this calibration, errors can be produced in the absolute value of the wind. Nevertheless, when doing spectral analysis the periods at which the energy peaks as well as the coherence obtained from cross-spectral analysis are not affected by the absolute calibration. On this basis it was decided to use the three time-series of ambient noise to determine the role of the forcing in the observed oceanic oscillation, but only in a qualitative way.

Low-frequency motion of the front

The location of the confluence front varies in time and space. In the analysis of the oscillations observed in the records, reference will be made constantly to the position of the front, and therefore it is important to recall how its location varies with time. In a recent paper, GARZOLI and GARRAFFO (1989) showed that the dominant motion of the front is an east–west displacement that, during the time covered by the observations, has a period close to one year. The position of the front along the line of deployment was determined from the analysis of the sounders' data, and results are shown in Fig. 2. According to this study, the mean position of the front from December 1984 to May 1985 ($\approx$6 months) fluctuates around $X = 0$ ($X = 0$ at the location of the onshore deployment IES 3; see Fig. 1). From July to December similar fluctuations occur around a mean

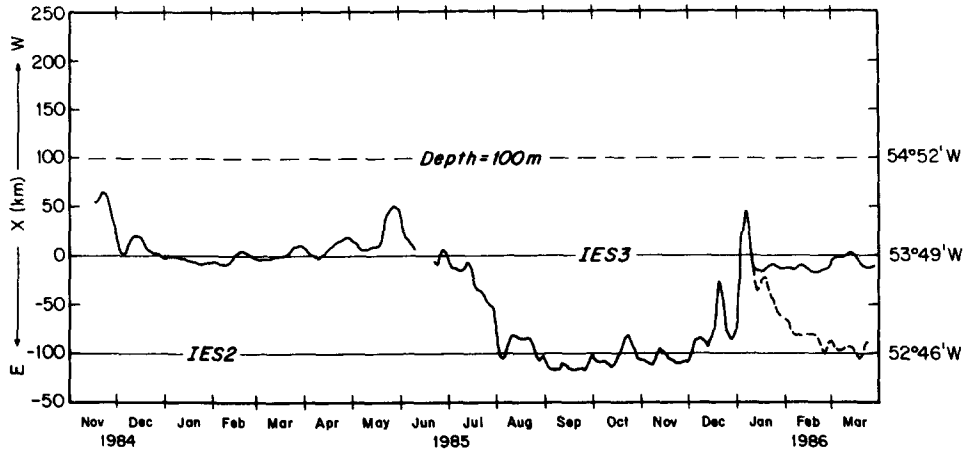

Fig. 2. Position of the front, X, as a function of latitude and time (adapted from GARZOLI and GARRAFFO, 1989). The proximity to the coast is represented by the depth contour = 100 m. Data is the result of a 5-day running mean average of the original hourly data.

position that is now displaced 100 km towards the east ($X = -103$ km). After this period of 6 months the front returns to $X = 0$. This low-frequency 100 km step motion is preceded in both cases by a rapid east–west displacement of the front: during November 1984 the front travels 70 km to the east ($X = 70$–0 km), on 20 May it moves 50 km towards the west. From 28 May to 5 August the front moves 150 km towards the east at an average speed of 2.2 km day^{-1} (2.5 cm s^{-1}). On 28 December 1985 the front starts a fast westward motion (14.4 km day^{-1} or 16.7 cm s^{-1}) towards $X = 40$ km. This suggests a 6-month oscillation superimposed on the main displacement of the front that has a time scale of 12 months. According to this analysis, during the second period of observations (June 1985 to March 1986) the front is located either at IES 3, IES 2 or between the two locations. The front never reaches the position of IES 1. An uncertainty in the front position occurs from 12 January 1986 to the end of the record. Each instrument indicated a different position of the front (dashed line in Fig. 2). That the front was located near $X = 0$ was decided on the basis of a simultaneous analysis of the dynamic height time-series at the three locations (GARZOLI and GARRAFFO, 1989). The records at this last location are characterized by a practically constant value of dynamic height and the observed anomalies correspond to the passage of cold or warm intrusions (GARZOLI and GARRAFFO, 1989).

Spectral analysis

The high-frequency oscillations present in the records are studied by means of spectral analysis techniques. Figure 3 shows the power density spectra (a) for the three simultaneous series of dynamic height. Spectral estimates are the result of a running mean over nine frequency bands. Significant peaks are observed at the tidal frequencies (diurnal and semidiurnal tides). The corresponding variance preserving spectra (b) show increases in the variance at different periods whose significance will be determined from the cross-spectral analysis between the records.

The slope of the power density spectra is a measurement of the energy in the ocean.

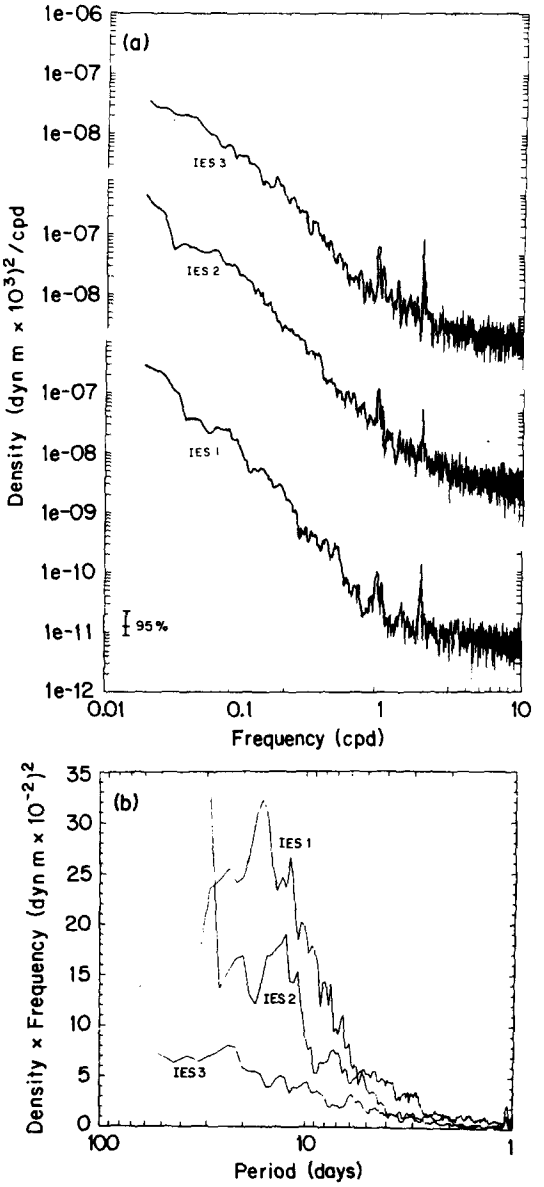

Fig. 3. Power density (a) and variance-preserving (b) spectra of the time-series of dynamic height at locations IES 3, IES 2 and IES 1. The error bar corresponds to the 95% confidence level.

Given the fact that the series under consideration are the first long-term observations obtained at the confluence, the observed spectral slope is compared to the one corresponding to other boundary currents or open ocean. For periods between 1 and 50 days the slope of the power density spectrum obtained at the western (IES 3), central (IES 2), and eastern (IES 1) locations is -2.29 ± 0.03, -2.40 ± 0.03 and -2.67 ± 0.03, respectively. These values are apparently higher than the universal one of -2.0 and show a tendency to

increase linearly from east to west. The slope of the power density spectra of the 17-month time-series at the offshore location is -2.90 ± 0.03, consistent with the previous statement. The apparent increase of the slope will be consistent with the local dynamics. An inspection of the three series (Fig. 1) shows that while the time-series of dynamic height obtained at the western location (IES 3) presents an approximate constant level with high-frequency oscillations superimposed on it, the central location (IES 2) also presents a strong 6-month oscillation. Instabilities of the front will produce a variability of the total energy, and therefore the position of the front will play a role in the total energy of the spectra: during the observed period the front was mostly located east of the onshore location (IES 3) and the central locations (IES 2, Fig. 2). The eastern location (IES 1) has important variations in dynamic height associated with the presence of cold intrusions (GARZOLI and GARRAFFO, 1989). The presence of eddies shed from the Brazil Current at the confluence is the determinant factor that increases the energy level at the offshore location; the available potential energy associated with these eddies is of the same order of magnitude as that calculated for the Gulf Stream's eddies (GARZOLI and GARRAFFO, 1989).

From spectral analysis of time-series collected at the Gulf Stream with inverted echo sounders, WATTS and JOHNS (1982) obtained values for the power density slope in the 2–4.16 day band period between -1 and -2 and of the order of -4 for periods larger than 4.16 days. The slopes for periods between 2 and 4.16 days and for periods greater than 4.16 days were calculated from Fig. 3 to compare with the values obtained at the Gulf Stream. For $2 < T < 4.16$ days the corresponding slopes are 2.81 ± 0.12, 3.22 ± 0.11 and 1.56 ± 0.12 at the westernmost, central, and easternmost locations, respectively. As will be seen later, the presence of the front causes energetic oscillations in this band. This will explain the fact of a larger slope at the intermediate location. The corresponding values for $T > 4.16$ days are 1.71 ± 0.04 (IES 3), 2.08 ± 0.05 (IES 2) and 2.16 ± 0.05 (IES 1). From the 17-month length record available at the IES 1 location, the slope resulted to be -1.3 ± 0.01 for periods between 2 and 4.16 days and -2.2 ± 0.03 for $T > 4.16$ days. The spectral slopes at the Brazil/Malvinas confluence zone are in agreement with those obtained for the Gulf Stream for periods between 2 and 4.16 days but the spectral slopes are lower for periods larger than 4 days, indicating that at those periods the Gulf Stream area is more energetic than the confluence.

Results from the spectral analysis of the wind magnitude squared at the three locations are given in Fig. 4a that shows the power density spectra and in Fig. 4b that shows the variance-preserving spectra at the three locations. Spectral estimates are again the running mean of nine frequency bands. The square of the wind magnitude is a quantity that has the same spectal properties as the wind stress. It is interesting to note when comparing these spectra (Fig. 4) with the ones obtained from the dynamic height records (Fig. 3), that for frequencies shorter than 0.1 cpd, the energy in the oceanic records increases toward lower frequencies, while for the atmospheric records, the energy levels off. The predominant feature of the wind spectra is the high level of variability in the 2–10 days band; in all the three spectra the energy increases at periods centered around 2, 3.3, 4.5 and 8 days. This is consistent with what is considered a typical spectra of the wind for latitudes poleward of 40° (e.g. OORT and TAYLOR, 1969). It is well known that fluctuations in the surface winds at mid-latitudes and high latitudes are most energetic in the frequency band from 2 to 10 days (PHILANDER, 1978). The energy in this band is associated with eastward-traveling cyclones which have a horizontal scale of the order of 5000 km (WILLEBRAND, 1977) and are the most distinctive feature of the atmospheric forcing at these latitudes (PHILANDER, 1978).

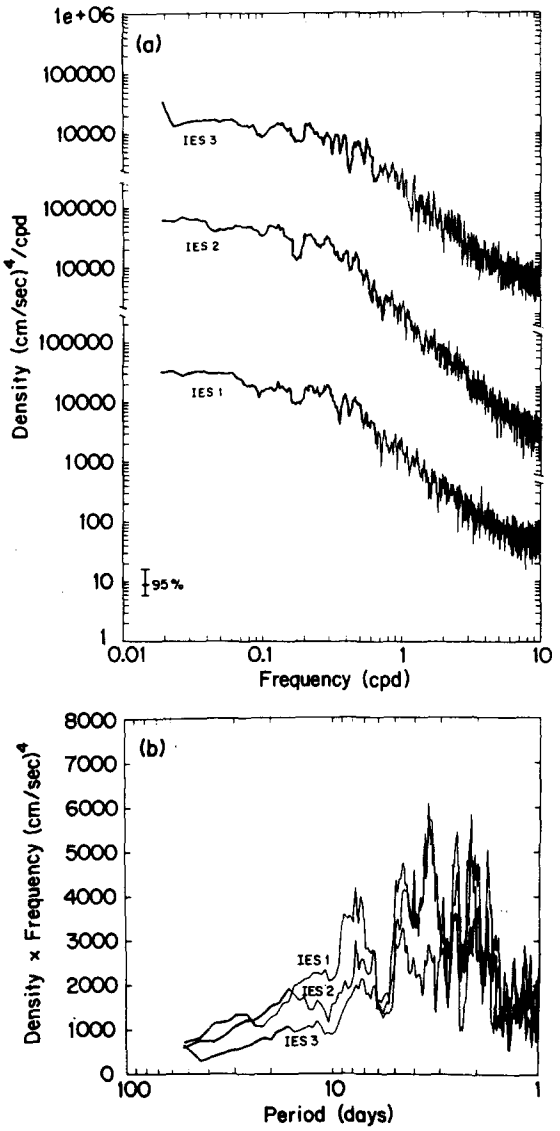

Fig. 4. Power density (a) and variance-preserving (b) spectra of the time-series of wind magnitude squared at locations IES 3, IES 2 and IES 1. The error bar corresponds to the 95% confidence level.

COHERENT OSCILLATIONS

The methods

To establish whether the oscillation observed can be related to physical processes, the coherence between records is analysed. Even though most of the peaks observed in the power spectras (Figs 3 and 4) might not be above the 95% confidence level, a significant level of coherence in amplitude and steadiness in phase from the cross-spectral analysis will indicate the presence of organized motion. On this basis, the cross-spectral analysis

between the different hourly sampled series (dynamic height and wind magnitude squared) was performed. Spectral estimates are the result of the running mean average of nine frequency bands. According to AMOS and KOOPMAN's (1963) tables, coherences are significant above 95% when greater than 0.40. The error in the phase is a function of the coherence. For coherence = 0.4 the error in the phase is ±25°. In this paper, the results of the cross-spectral analysis as a result of nine frequency bands averaging are shown. But, in all of the cases when an oscillation is under consideration for interpretation of a physical process, the analysis is repeated for larger averaging to see if the coherence above the level of confidence persists. Only if it passes this test is it taken into consideration.

A useful method to analyse the coherence between more than two records is the empirical orthogonal functions (EOF) analysis in the frequency domain (WALLACE and DICKINSON, 1972). In the case under analysis, three or six time-series, it is mostly useful to present the results and to determine when, at a certain period, an oscillation is present in all or most of the records. From the coherence matrix between the different series the eigenvalues (λ_i) and eigenvectors (e_{ij}) are calculated. The empirical modes are determined from these values as well as the percentage of variance explained by each mode (% VAR) and the fraction of variance explained by the ith variable at the jth mode (γ_{ij}). This last one is, by definition, the square of the coherence between the variable and the mode at each site.

Once the different modes characterized by their eigenvectors (e_{ij}) and eigenvalues (λ_i) are determined, it is necessary to establish whether they represent a true signal of physical significance or if they cannot be differentiated from the noise. A powerful selection criteria is given by PREISENDORFER *et al.* (1981), who presented a Monte Carlo technique for selection of principal components for which the geophysical signal is greater than that of the level of noise. The level of noise is simulated by repeated sampling of principal components computed from a spatially and temporally uncorrelated random process. The rule has been found to be relatively robust and conservative, and it has been tabulated by OVERLAND and PREISENDORFER (1982). In this paper the 95% significance level for the first two modes is determined on the basis of a smooth curve fitting of the tabulated values. Only points lying above their respective significance level can be considered statistically significant. One should note, however, that the tabulated values are derived from the correlation matrix and are expected to vary slightly, but still remain as conservative, when a covariance or cross-spectral density matrix is used (OVERLAND and PREISENDORFER, 1982). Another selection criteria concerns the sample variance of the eigenvectors. Following NORTH *et al.* (1982) the sampling error of a particular eigenvalue λ_i can be estimated as $\delta\lambda_i = \lambda_i \times (2/N)^{1/2}$, where N is the number of independent realizations of the field. If the sampling error of a given eigenvalue λ_i is smaller than the spacing between λ_i and a neighboring eigenvalue (λ_{i-1} or λ_{i+1}), then the corresponding modes can be separated and physically interpreted.

On these bases, to study the simultaneous coherences in all the frequency bands present in the oceanic records, the three 9-months dynamic height time-series are decomposed into empirical orthogonal modes in the frequency domain. Period bands of significant coherence are determined from the results. Their significance is established by the error analysis and by the cross-spectral analysis. To determine whether an oceanic oscillation is free or wind forced, cross-spectral analysis and the EOF analysis in the frequency domain are performed for the three simultaneous oceanic and wind magnitude squared records. To give equal weight to the measurements at different sites or of different kinds (dynamic

height and wind magnitude at three different sites), the cross-spectral matrix is normalized by dividing each element by the product of the square root of the variance associated with each member of that pair.

To analyse a possible relation between the oscillations observed and the presence of the front, we study the relation between the position of the front (X, Fig. 2) and the dynamic height series at the offshore location (DH_1, Fig. 1) by means of cross-spectral analysis. The position of the front, X, determined from a non-linear relation between the depth of the 8°C isotherms at IES 3 and 2 (GARZOLI and GARRAFFO, 1989), was found never to reach the position of IES 1 (the offshore location) during the observed period of time. Therefore, a significant coherence between the two time-series (X and DH_1) in that frequency band might indicate that its origins are in the east–west displacement of the front.

Results from the EOF analysis of the three dynamic height time-series (Fig. 5a and Table 2) show the percentage of variance explained by the two dominant empirical modes as a function of the period. The horizontal lines indicate the 95% significance level for the first two modes from the test for randomness based on a smooth curve fitting the tabulated values of OVERLAND and PREISENDORFER (1982). According to this rule, attempts at physical interpretation of a mode 1 are valid if the ratio between the variance explained by the mode and the corresponding value of a random-generated (U_j^{95}) is larger than one. In the cases under consideration, the values of U_j^{95} (for j = mode number = 1 and 2 at 95% confidence level) are: $U_1 = 48.50$ and $U_2 = 32.70$ for three time-series and nine frequency bands and $U_1 = 37.00$, $U_2 = 27.50$ for six time-series and nine frequency bands. Brackets are examples of the sampling errors according to NORTH *et al.* (1982).

Table 2 shows examples of those periods for which the first empirical mode is significant and correlated to (almost in all cases) the three locations. This is shown by the fraction of variance explained by the ith variable at the jth mode (γ_{ij}). Note that this latter variable is by definition, the square of the coherence between the variable and the mode (WALLACE and DICKINSON, 1972). For nine frequency bands the significant level of coherence at 95%

Table 2. Some examples of EOF analysis in the frequency domain of the three oceanic records. The table displays for different periods, the percentage of variance explained by the first mode (% VAR) *and the square of the coherence between the variable and the mode* (γ_{ij})

Mode 1 Period (days)	% VAR	γ_{ij} IES 3	IES 2	IES 1
37.4	57.2	**0.54**	**0.47**	**0.70**
29.1	59.7	**0.51**	**0.46**	**0.82**
11.9	60.3	**0.61**	**0.40**	**0.80**
6.09	57.2	**0.08**	**0.80**	**0.85**
5.04	71.8	**0.70**	**0.84**	**0.61**
4.85	61.7	**0.61**	**0.68**	**0.56**
3.16	58.4	**0.44**	**0.55**	**0.77**
2.40	58.6	**0.56**	**0.62**	**0.58**
2.16	65.0	**0.60**	**0.71**	**0.67**
2.03	68.8	**0.76**	**0.79**	**0.52**

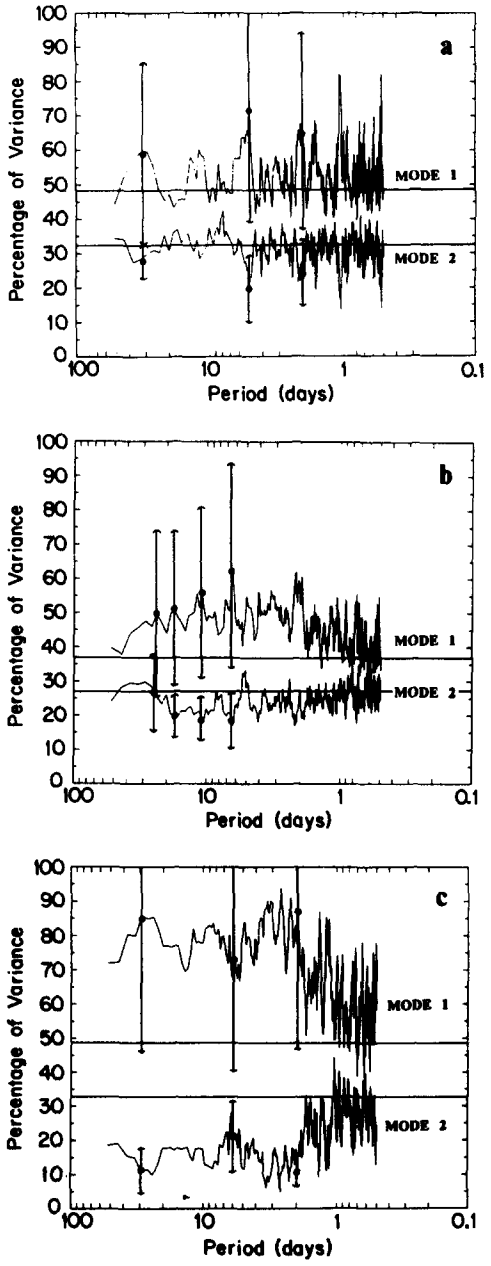

Fig. 5. Percentage of variance explained by the first and second empirical modes as a function of period from the EOF analysis in the frequency domain for: (a) the three time-series of dynamic height; (b) the three time-series of dynamic height and the three time-series of the magnitude of the wind squared; and (c) the three time-series of the magnitude of the wind squared. Horizontal lines indicate the 95% confidence limit for the first two modes from the test from randomness. Brackets are examples of the sampling errors of the eigenvectors

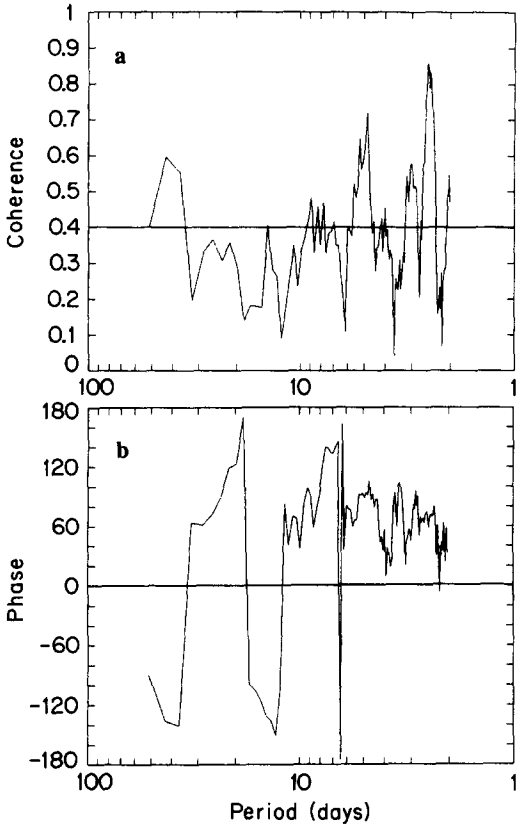

Fig. 6. Coherence in amplitude (a) and phase (b) from the cross-spectral analysis between the time-series distance to the front (X) and the dynamic height at the offshore location (IES 1). Horizontal line in the coherence panel (a) indicates 95% confidence limit.

is 0.40. Values in bold indicate that the higher coherence observed, $(\gamma_{ij})^2$, is with the first mode.

Results of the EOF analysis of the combined dynamic height and wind magnitude squared records (Fig. 5b) show the percentage of variance explained by the two first dominant modes as a function of period. Solid lines indicate the levels above which the modes are significant. Brackets are examples of the sampling errors according to NORTH *et al.* (1982). Figure 5c shows the same results from the empirical decomposition of the three wind magnitude squared (W^2) records only. The coherence in amplitude and phase from the cross-spectral analysis between the position of the front (X) and the dynamic height series at the offshore location (DH_1) are shown in Fig. 6.

The analysis

Coherent oscillations might be wind forced or their origin might by traced to the local ocean dynamics of the area determined by: the existence of a continental shelf that through the mechanism of high depth gradient can originate topographic Rossby waves; the

presence of the thermohaline front and its associated east–west displacement; and the meandering of the Brazil Current after the confluence.

The data have been analysed in the following bands; from 20 to 55 days, 10 to 15 days and 2 to 10 days, based on all previous cross-spectral and EOF results. Each of these bands has the following characteristics in common: (1) oscillations in the first empirical mode can be distinguished from noise, based upon the criterias discussed above, indicating the possibility of physical processes present in the records; (2) they are significantly coherent either to the wind magnitude squared records or to the position of the front. Due to their specific characteristics and method of analysis, the tidal signal is studied in a separate note.

Band from 20 to 55 days. Even though from the EOF analysis (Fig. 5a) it would appear that the oscillations found in the 20–55 days band all represent the same phenomena, the cross-spectral analysis between the position of the front and the dynamic height at IES 1 (Fig. 6) shows that the band is divided into two parts: from 36 to 52 days, the records are significantly coherent; maximum coherence is obtained at periods centered at 37.4 days. On the other hand, for periods between 20 and 31 days (a band that from the EOF contains the maximum percentage of variance explained by the first empirical mode, 59.7% at 29.1 days), the coherence between X and DH_1 is below the confidence level. Therefore it can be assumed that there are two different oscillations in this band with different origins, and they will be analysed separately.

(a) Periods centered at 37.4 days.

Results from the EOF analysis (Table 2) show that for periods centered at 37.4 days, the first mode is significantly coherent to the three oceanic records obtained at the IES 3, 2 and 1 locations; 57.2% of the total variance of the system can be explained by this mode. The amplitude of the oscillation, defined as $A_{ij} = \lambda_i^{1/2} \sigma_j e_{ij}$ (where λ_i is the eigenvalue, e_{ij} is the eigenvector and σ_j is the standard deviation) and the phase (determined from the complex eigenvector) are obtained. For $T = 37.4$ days, the computed amplitudes at IES 3, 2 and 1 are, respectively, 0.07, 0.18 and 0.24; the corresponding phases are 0, −159 and −249 (with an error lower than ±15°). A linear regression for the phase lag between the three locations indicates the presence of a wave propagating westward with a wavelength [$\lambda = d^* 2\pi/(\phi \pm 2n\pi)$, where d is the distance between stations and ϕ is the phase lag] of −258 km (±24 km) for $n = 0$ and −150 km (±24 km) for $n = 1$. The corresponding phase speed of propagation is −8.0 cm s^{-1} (or −6.9 km day^{-1}) and −4.6 cm s^{-1} (or −4.0 km day^{-1}), respectively. Therefore 57.2% of the variance of the system at periods centered at 37.4 days can be explained by a wave that propagates westward with amplitude that increases linearly towards the east. The sense of the phase propagation observed for this oscillation (westward) is compatible with the one corresponding to baroclinic Rossby waves (BRW). Nevertheless, it can be shown (e.g. GILL, 1982) that BRW can only exist at a given latitude ϕ for periods that satisfy the relation

$$T \geq 4\pi R \tan \phi/(gh_r)^{1/2}, \tag{1}$$

where R is the radius of the Earth, g is the acceleration of gravity and h_r is the equivalent depth. For the area under analysis, the equivalent depth corresponding to the gravest baroclinic mode ($r = 1$) is 0.7 m (GARZOLI and BIANCHI, 1987); according to equation (1) the minimum period for BRW to be generated at these latitudes is approximately 270 days,

much larger than the observed 37.4 days. A BRW can exist at those periods (T = 37.4 days) only up to a maximum latitude of approximately 8° (equation 1). Therefore the basic theory for baroclinic Rossby waves does not support the observations. At these latitudes and with periods similar to the one observed, the theory does predict the existence of barotropic Rossby waves. Nevertheless, it is well established (WATTS and ROSSBY, 1977; GARZOLI and KATZ, 1981) that IES instruments are only detectors of low baroclinic modes. From all of the above, it can be concluded that the oscillation observed at periods centered at T = 37.4 days cannot be a Rossby wave.

To determine whether the oscillation is forced by the winds, results from the cross-spectral and EOF analysis of both oceanic and atmospheric records are analysed (Fig. 5b). For periods centered at 37.4 days, the analysis indicates that the two first empirical modes take into account 73.8% of the total variance of the system. The confidence level estimated for each of these modes (U_1 = 37.00 and U_2 = 27.50) indicates that they are statistically significant, but the errors in the eigenvector do not allow us to separate the modes. Therefore, we analyse the individual coherences between the oceanic records and W^2. For periods centered at 37.4 days, the coherences are: 0.44, 0.47 and 0.24 for IES 3, 2 and 1, respectively. Since the coherence with the wind is small and not observed at the three locations it is possible to assume that the oscillation at periods centered at 37.4 days is not primarily wind forced.

For periods between 36 and 52 days, the coherence level between the position of the front and the dynamic height at the IES 1 location is significant and reaches a maximum value of 0.60 at 42.8 days (Fig. 6). This is interpreted as an indication that the oscillation is due to the presence of the front. LEGECKIS and GORDON (1982) observed from satellite infra-red images of the Brazil and Malvinas currents that the warm water associated with the Brazil Current fluctuates southward and northward between 38° and 46°S with a time scale of about 2 months. This is close to the period of the wave observed with the sounder records. Therefore, it is possible to assume that the oscillation that corresponds to a westward-propagating wave with a period centered at 37.4 days is not forced by the wind but is related to the motion of the front.

(b) Periods centered at 29.1 days

The previous analysis (Table 2) shows that for periods centered at 29.1 days, the first mode is highly coherent with the three oceanic records obtained at the IES 3, 2 and 1 locations. The resulting amplitudes of the oscillations are 0.06, 0.11 and 0.72, respectively, with corresponding phases of 0°, 174° and 257°. The error of the phase estimate is less than ±15°. These values indicate the presence of a wave that propagates eastward with a wavelength of 250 km (±24) for n = 0 and 140 km (±24) for n = 1. The corresponding phase speed of propagation is 10.0 cm s^{-1} (or 8.6 km day^{-1}) and 5.6 cm s^{-1} (or 4.8 km day^{-1}), respectively. That is to say, the wave propagates eastward with a linear increase of its amplitude and phase in the offshore direction.

That the oscillation is not forced by the winds can be deduced from similar considerations as in the previous section. Coherence between the dynamic height and the square of the wind magnitude is 0.15, 0.37 and 0.28 for IES 1, 2 and 3, respectively.

Therefore, at periods T = 29.1 days, a wave is observed with characteristics similar to the one observed at T = 37.4 days but that propagates in the opposite direction. Neither of these waves shows indications that they are forced by the winds. While the westward-propagating wave can be attributed to the motion of the front, no indication is observed

that this is the case for the wave with periods centered at 29.1 days. In what follows, the different mechanisms that may cause this 29.1-day period wave will be explored.

Topographic Rossby waves (TRW) have been observed in the Gulf Stream, an area that is characterized by dynamics that are similar to those of the confluence. From current meter data collected in the Gulf Stream, THOMPSON (1977) obtained good agreement between observed phase propagation of motion at periods of 8, 11, 16 and 32 days and those predicted by RHINES' (1970) linear bottom-trapped topographic wave model; for a period of 32 days he observed phase velocities of 7–8 km day^{-1} and wavelength of the order of 250 km. HOGG (1981), from a similar data set, also collected in the Gulf Stream at 70°W between 36° and 40°N, analysed oscillations in three period bands: 22–108, 12–22 and 8.3–12 days. With a few exceptions, the horizontal phase variations and vertical energy decay away from the bottom are well described in each of the three frequency bands by a simple topographic wave propagating offshore and refracting in response to changes in the environment. In the same region JOHNS and WATTS (1986), on the basis of observations of the current and temperature variability, concluded that at levels shallower than approximately 1500 m, temperature variations in the period band from 2 to 48 days are dominated by spatially coherent displacement of the thermal structure, associated with the meandering of the path of the Gulf Stream. However, at low frequencies (periods of 24–48 days), the meander-dominated regime in the upper layer gives way to an essentially uncoupled TRW variability below about 2000 m. They established that TRW were energetically dominant at periods longer than 14 days and found at a period band centered at 32 days a fluctuation characterized by offshore propagation, with a phase speed of propagation 6.9 km day^{-1} and wavelength 220 km which was consistent with the theoretical properties of TRW. In a stratified fluid baroclinic TRW dynamics play an important role in the low-frequency motions of the continental slope (OU and BEARDSLEY, 1980). The possible mechanism for generation of TRW in the Gulf Stream has been suggested to be the rings that are shed by the main flow (LOUIS and SMITH, 1982) and the forcing of the large meanders (HOGG, submitted).

Our results show that the parameters that characterize the oscillation—period (centered at $T = 29.1$ days), wavelength (250 km) and sense of phase propagation (offshore)—are similar to those observed in the Gulf Stream and associated to TRW. In addition, the characteristics of the region, both dynamic and bathymetric, are such that the generation of TRW is possible. Nevertheless, TRW are assumed to be bottom trapped and the temperature signal at the level of the thermocline, very small. If this is the case, their detection with the IES is almost impossible. In order to determine if, given the characteristics of the confluence, TRW are bottom trapped, the vertical structure of the oscillation's amplitude is analysed using a simple theoretical model in the presence of stratification (e.g. PEDLOSKY, 1979). The dispersion relation for these waves is

$$\omega = -\Gamma N l/(l^2 + k^2)^{1/2}, \tag{2}$$

where Γ is the bottom slope, N is the Brunt–Väisälä frequency and k and l are the wavenumbers in the zonal and meridional directions, respectively. From this relation it follows that for typical values of Brunt–Väisälä frequency (1–2 cph) and bottom slope (0.02) TRW can exist at the observed periods. The vertical amplitude of these waves is of the form

$$\Phi(z) = A \exp(-z/d*) \quad (z = 0 \text{ at the bottom}). \tag{3}$$

This amplitude decays away from the bottom with an e-folding scale, $d*$, equal to $\lambda f/2\pi N$ (where λ is the wavelength and f the Coriolis parameter). According to the definition of $d*$, largely stratified areas, with large values of N, will have a very small e-folding and the waves will be strongly bottom trapped. In the other extreme, homogeneous regions with a value of N close to zero will be characterized by an e-folding much larger than the depth of the ocean and the resulting waves will be nearly barotropic. In order for these waves to have a significant signal in the temperature at the level of the thermocline the values of $d*$ should be of the order of magnitude of the depth of the ocean. If this is so, the waves can be clearly detected by the echo sounders. From the Brunt–Väisälä frequency obtained from the CTD casts, the average values of $d*$ are of the same order as the depth of the ocean H, for H ranging from 1000 to 2000 m. For H between 2000 and 5000 m the value of $d*$ decays to 50% of the ocean depth. In any case, the waves will have a signal detectable with the sounders.

Therefore, the oscillations at periods $T = 29.1$ days can be attributed to topographic Rossby waves. As was shown before, for period centered at 29.1 days (Fig. 6), there is no coherence between the motion of the front and the dynamic height at the offshore location. A plausible explanation is therefore that the waves must be forced by the meandering of the current. It is well known that the Brazil Current, after initial overshoot, meanders northeastward toward subtropical latitudes; the meanders have a wavelength of about 400 km and an amplitude of 200 km (RODEN, 1986). Meanders at these periods have been repeatedly observed in the Gulf Stream (WATTS and JOHNS, 1982; JOHNS and WATTS, 1985, 1986).

Therefore, in the 20–55 day band, the observations support the existence of two waves that propagate at different periods (37.4 and 29.1 days) in opposite directions, with similar wavelength and phase speed of propagation. No evidence is found to suggest that these waves are forced by the atmosphere. The westward-propagating wave appears to be forced by the presence of the front while the eastward-propagating wave has all the characteristics of TRW forced by the meandering of the current.

Band from 10 *to* 15 *days*. The second band to be analysed is from 10 to 15 days. No significant coherence is observed between the position of the front and DH_1 in this frequency band (Fig. 6). It appears that the oscillation observed at the offshore location (IES 1-O) is wind forced, while at the onshore location it has a different origin. This is derived from the results of the individual cross-spectral analysis between the different pairs of dynamic height and wind records. Significant coherence is observed (0.52–0.60) at IES 1. There is no coherence at the other two locations, with the exception of periods of 11.9 days where a coherence of 0.43 is observed between the ocean and the atmosphere at IES 3. Therefore, in this band the observations support the existence of a wind-forced oscillation that has maximum amplitude at the offshore location. Also observed in this band is an oscillation at very similar periods that appears only at the onshore location and that might be due to the presence of the coast.

Band from 2 *to* 10 *days*. The EOF analysis (Fig. 5a and Table 2) of the three 9-month long oceanic records, suggests the existence of coherent oscillations for different periods in the 2–10 day band. This is also valid for the atmospheric records represented by the square of the wind magnitude, W^2. In this latter case, most of the energy of the spectra is

concentrated in the 2–10 day band (Fig. 5b) and the oscillations are highly coherent (Fig. 5c). It is well known that the mid- to high-latitude wind spectra present high levels of energy in this band and the origins are attributed to eastward-traveling cyclones (OORT and TAYLOR, 1969). It is also known that in frontal zones, like in the Norwegian Current (MYSAK and SCHOTT, 1977) and the Antarctic Circumpolar Current (BRYDEN and PILLSBURY, 1977; BAKER *et al.*, 1977), the spectra of the current present a considerable amount of low-frequency variability due to barotropic and baroclinic instabilities. Oscillations in this band were also observed in the Gulf Stream. WEBSTER (1961) observed oscillations in the offshore position of the Gulf Stream at periods of 6.9, 3.9 and 2.7 days. BROOKS and BANE (1981) confirmed these observations and reported neither correlation to the winds nor to the pressure field. Oscillations are attributed to a possible baroclinic instability. WATTS and JOHNS (1982) reported meander-associated motions in this band (from 4 to 10 days) and also suggested that the origin can be traced to baroclinic instabilities.

If the oscillations observed in the atmosphere in these bands are due to the eastward-traveling cyclones, they would be expected to exhibit a variability in the level of energy with the season: the level of energy should be higher during winter and spring and lower during autumn and summer. To determine seasonal variability in the energy contained in this band, the records are divided by seasons and the results analysed. The analysis was done with the record from IES 1 where a time-series of 17 months long is available providing the possibility of determining the seasonal variability with better resolution and for all of the seasons. The examples presented in this section therefore correspond to the offshore location. The same analysis performed at the two other locations (not shown) with shorter records confirms the results.

Figure 7 shows the spectral analysis (variance preserving) of the wind square (a) and dynamic height (b) time-series for five consecutive seasons (seasons correspond to the southern hemisphere): (1) summer 1984–1985, (2) autumn 1985, (3) winter 1985, (4) spring 1985 and (5) summer 1985–1986. The series were previously passed through a band pass filter that eliminates periods outside the 2–10 days band. Even though not in the expected order, the wind spectra show a seasonal variability; for example, at periods centered at 2 days, the energy is one order of magnitude higher in autumn 1985 than in the summer of 1984–1985. An interannual variability is also observed between the two analysed summers. In addition to this variability in the level of energy it is interesting to note that while during autumn, winter and spring the spectrum of the wind is bimodal (two peaks centered at around 4 and 2 days), during the summer it becomes unimodal.

The variance-preserving spectra of the ocean also show a marked seasonal variability (Fig. 7b): minimal during the two observed summers and autumn and maximal during the winter and spring. Contrary to what happens in the wind spectra, the inter-annual variability is almost negligible. It is interesting to note that when comparing the results from the wind and oceanic records (Fig. 7a,b) there is a difference in the distribution of energy with period: in the ocean the energy is shifted towards lower frequencies than the one observed in the wind records; the maximum in energy is observed between 4 and 8 days. This is to be expected since the relation between the forcing function and the oceanic response is inversely proportional to the frequency. That is to say, even in the event that the forcing would be constant with frequency, the oceanic spectra of the response will be more energetic at low frequencies. Nevertheless, even though the energy observed in the wind spectra in the 2–10 day band might be due to the eastward-traveling cyclones, due to the differences noted in the seasonal variability it can be assumed that the oscillations

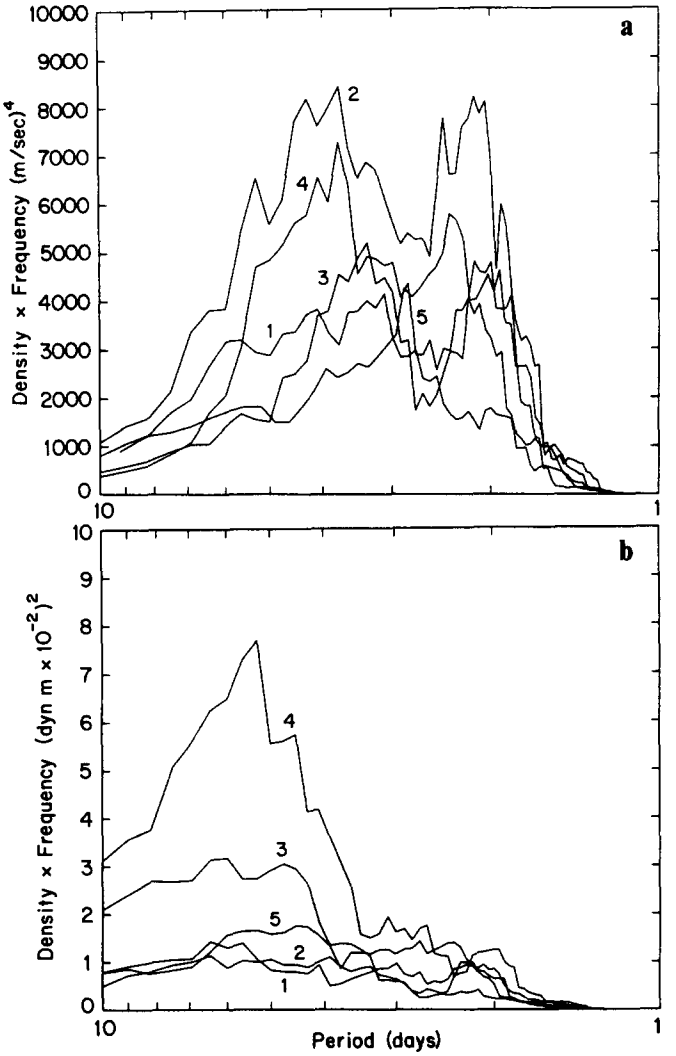

Fig. 7. Variance-preserving spectra of (a) the magnitude of the wind squared and (b) dynamic height for (1) summer 1984–1985, (2) autumn 1985, (3) winter 1985, (4) spring 1985 and (5) summer 1985–1986.

observed in the oceanic records are only partially forced by the wind. Most of the energy in the 2–10 day period band must have a different origin.

To determine the origin of the oscillations in this band we analysed simultaneously the coherence between the ocean records, between the position of the front and the dynamic height at the offshore location and the coherence between the ocean and the wind magnitude squared. The analysis is done in a similar way to the one described in the previous sections: by cross-spectral analysis as well as EOF analysis in the frequency domain of the six time-series (three from oceanic records and three from wind magnitude squared measurements). The results from these analyses will now be described.

In the band from 5.5 to 10 days, the EOF decomposition of the oceanic records shows

that the first mode is correlated to the two offshore locations while oscillations observed in the onshore location are correlated to a second mode (see Table 2 for an example). Only at periods between 9 and 10 days are the modes statistically separable. The cross-spectral analysis between the position on the front and the dynamic height series at the offshore location presents some peaks of coherence in this band, but they are narrow and when averaged, in the limit of significance (Fig. 6). Coherence is observed between the ocean and W^2 at the offshore location. Therefore, no significant conclusions can be derived from the oscillations in this band. If any, the wind is forcing the ocean at the two offshore locations.

The situation is different for periods between 5.5 and 2 days. There is a significant first mode correlated to the three oceanic records (Table 2); the percentage of variance explained by this empirical mode can be as high as 71.8% and in all cases the coherence between the oceanic records and the mode is higher than $r = 0.66$ ($r^2 = \gamma_{ij} = 0.44$). The band is analysed by the methods described before and the results are summarized in Table 3.

From the cross-spectral and EOF analysis of the combined series it is possible to establish that the wind is forcing the ocean at periods between 5.0–5.2 days and 2.1–2.3 days. In both cases, there is significant coherence between the wind and the ocean (Table 4). For periods from 5.2 and 5.0 days, there is also a correlation with the position of the front (Fig. 6), which might be an indication of a combined mechanism.

For periods between 3.4 and 3.9 days, even though there is a significant coherence between the three oceanic records (Table 3) no coherence is found either with the wind (not shown) or the position of the front (Fig. 6). The origin of the oscillations observed in the ocean cannot be explained with the present analysis.

There are other oceanic oscillations that show no significant coherence to the wind, but a high coherence with the position of the front. This is the case for periods 4.6–5.0, 3.0–3.4, 2.3–2.6 and 1.9–2.1 days (Table 3). These oscillations are assumed to be forced by the baroclinic instabilities that originate from the presence of the front and its motions. This can be confirmed by comparison of Fig. 2, which shows the position of the front as derived by GARZOLI and GARRAFFO (1989), with Fig. 7b, which shows the seasonal variability of the energy level of the ocean at the offshore locations (IES 1). It becomes evident that: (1) during the summer of 1984–1985, when the front is located at the onshore location (IES 3),

Table 3. *Resume of the results in the* 2–5 *day period band*

Band	Coh. (X, DH_1)	Coh. (W^2)	Origin
5.2–5.0	>0.56	Yes	Wind
2.3–2.1	No	Yes	Wind
3.9–3.4	No	No	Free?
5.0–4.6	>0.58	No	Front
3.4–3.0	>0.45 (0.58)	No	Front
2.6–2.3	>0.51 (0.86)	No	Front
2.1–1.9	>0.4 (0.55)	No	Front

Columns are: the band period; coherence between the position of the front and the dynamic height at the offshore location; coherence between dynamic height and W^2; and a possible explanation of the origin of the oscillations.

Table 4. Results from the EOF analysis as a function of the mode number for periods centered at 5.04 days and 2.20 days

Period = 5.04 days Mode no.	% VAR	γ_{ij} IES 3-O	IES 2-O	IES 1-O	IES 3-W^2	IES 2-W^2	IES 1-W^2
1	55.2	**0.47**	**0.47**	**0.50**	**0.64**	**0.76**	**0.47**
2	20.0	**0.40**	**0.40**	0.14	0.28	0.08	**0.38**
3	8.6	0.07	0.03	**0.33**	0.01	0.01	0.06

Results from the EOF analysis in the frequency domain of the three oceanic records (IES-O) and the square of the magnitude of the wind (IES-W^2). The table displays for periods centered at 5.04 days, the percentage of variance explained by the first three modes (%VAR) and the square of the coherence between the variable and the mode (γ_{ij}) at each different location.

the energy level of the spectra in this band at IES 1 is low; (2) during the autumn, when the front is located west of IES 3, the energy in the spectra at IES 1 reaches a minimum value; (3) during the winter, the front is moving toward the central location (IES 2) and the energy in the spectrum at IES 1 increases; (4) maximum energy is observed at IES 1 in the spring when the front reaches the closest position to this station; (5) the energy level in the 2–10 day band at IES 1 decreases again during the summer of 1985–1986 when the front moves back to the onshore location (IES 3).

This is a very interesting result that confirms the hypothesis that there are oscillations in this band due to the presence of the front. Therefore, from the previous analysis we can conclude that the oscillations observed in the oceanic records in the band from 2 to 10 days are of different origins. Some of them are forced by the winds, others are due to the presence and motion of the front and the associated baroclinicity.

SUMMARY OF CONCLUSIONS

The analysis of the dynamic height records obtained at the Brazil/Malvinas confluence show that the motion of the front not only alters the low-frequency dynamics of the system, but is also a source of wave generation. These waves are part of the local dynamics and, therefore, it is important to determine their characteristics and origins. The waves interact with the main flow and should therefore be taken into consideration when studying the local dynamics and in any attempts to model the front or confluence region.

The main mechanisms for the origin of the observed oscillations can be found both in the atmosphere and the ocean. The first mechanism is the wind stress at the ocean surface. Traveling cyclones force the ocean at periods in the band from 2 to 10 days. These cyclones are assumed to have a seasonal variability. The present observations show that the spectral energy level in the atmosphere during spring is three times greater than in summer and autumn; in the ocean, this energy variation is as high as one order of magnitude.

The second forcing function at high-frequency levels is the confluence region itself, where the dynamics are determined by (a) the meandering that originates at the point of encounter of the two currents; (b) the displacement of the front due to a variability in the latitude of separation from the coast of the Brazil Current; (c) the topography, which because of a sharp slope, is the source of topographic waves; and (d) the drastic changes in

the vertical density structure of the water column that create the conditions for the generation of baroclinic instabilities.

In the band from 20 to 50 days the observations support the existence of two waves that propagate at different periods and in opposite directions with very similar characteristics but of apparently different origins: (1) a westward-propagating wave whose origin can be attributed to the north–south displacement of the front; and (2) a topographic Rossby wave that propagates eastward and which might be forced by the meandering of the Brazil Current. In the band from 2 to 10 days the cyclones are not the only forcing function of the ocean. Results show that the change in the vertical density structure, caused by the presence of the thermohaline front, produces instabilities which in turn generate waves (baroclinic instabilities).

Acknowledgements—This program was part of the Office of Naval Research, Southern Oceans Accelerated Research Initiative. The authors wish to thank Dr Kenneth Hunkins and Hsien Wang Ou for reviewing the manuscript. Mark Edwards performed the computer programing for data analysis and plotting. Susan Brower collaborated with the typing and final version of the manuscript. The participation of C. Simionato in the data analysis was supported by a grant from the Tinker Foundation to Lamont CU00327801 and a fellowship from the National Research Council of Argentina (CONICET). This research was supported by grants ONR N00014-87-K-0204 and NSF OCE 87-11529. This is LDGO contribution no. 4618.

REFERENCES

Amos D. E. and L. H. Koopmans (1963) Tables of the distribution of the coefficient of coherence for stationary bivariate gaussian processes. Sandia Corp, publ. SCR-483, 143 pp.

Baker J., W. D. Nowlin, R. D. Pillsbury and H. L. Bryden (1977) Antarctic circumpolar current: space and time fluctuations in the Drake Passage. *Nature*, **268**, 696–699.

Brooks D. A. and J. M. Bane (1981) Gulf Stream fluctuation and meanders over the Onslow Bay upper continental slope. *Journal of Physical Oceanography*, **11**, 247–256.

Bryden H. L. and R. D. Pillsbury (1977) Variability of deep flow in the Drake Passage from year-long current measurements. *Journal of Physical Oceanography*, **7**, 803–810.

Garzoli S. L. and E. J. Katz (1981) Observations of inertia-gravity waves in the Atlantic from inverted echo sounders during FGGE. *Journal of Physical Oceanography*, **11**, 1463–1473.

Garzoli S. L. and M. Clements (1986) Indirect wind observations in the southwestern Atlantic. *Journal of Geophysical Research*, **91**, 10551–10556.

Garzoli S. L. and A. Bianchi (1987) Time–space variability of the local dynamics of the Malvinas–Brazil Confluence as revealed by inverted echo sounders. *Journal of Geophysical Research*, **92**, 1914–1922.

Garzoli S. L. and Z. Garraffo (1989) Transports, frontal motions and eddies at the Brazil–Malvinas Currents confluence. *Deep-Sea Research*, **36**, 681–703.

Gill A. E. (1982) *Atmosphere–ocean dynamics*. International Geophysics Series, Vol. 30, W. L. Donn, editor, 662 pp.

Gordon A. (1989) Brazil–Malvinas Confluence—1984. *Deep-Sea Research*, **36**, 359–384.

Hogg N. (1981) Topographic waves along 70W on the Continental Rise. *Journal of Marine Research*, **39**, 627–649.

Johns W. and D. Watts (1985) Gulf Stream Meanders: Observations on the deep currents. *Journal of Geophysical Research*, **90**, 4819–4832.

Johns W. and D. Watts (1986) Time scale and structure of topographic Rossby waves and meanders in the deep Gulf Stream. *Journal of Marine Research*, **44**, 267–290.

Knudsen V. O., R. S. Alford and J. W. Emling (1948) Underwater ambient noise. *Journal of Marine Research*, **7**, 410–429.

Legeckis R. and A. Gordon (1982) Satellite observations of the Brazil and Falkland Currents—1975 to 1976 and 1978. *Deep-Sea Research*, **29**, 275–401.

Lemon D. D., D. M. Farmer and D. R. Watts (1984) Acoustic measurements of wind speed and precipitation over a continental shelf. *Journal of Geophysical Research*, **89**, 3462–3472.

LOUIS J. P. and P. C. SMITH (1982) The development of the barotropic radiation field of an eddy over a slope. *Journal of Physical Oceanography*, **12**, 56–73.

LUYTEN J. (1977) Scales of motion in the deep Gulf Stream and across the continental rise. *Journal of Marine Research*, **35**, 49–74.

MYSAK L. and F. SCHOTT (1977) Evidence for baroclinic instability of the Norwegian Current. *Journal of Geophysical Research*, **82**, 2087–2095.

NORTH G. R., T. L. BELL, R. F. CAHALAN and F. J. MOENG (1982) Sampling errors in the estimation of empirical orthogonal functions. *Monthly Weather Review*, **110**, 699–706.

OORT A. and A. TAYLOR (1969) On the kinetic energy spectrum near the ground. *Monthly Weather Review*, **97**, 623–636.

OLSON D., G. PODESTA, R. EVANS and O. BROWN (1988) Temporal variations in the separation of Brazil and Malvinas currents. *Deep-Sea Research*, **35**, 1971–1990.

OU H. W. and R. C. BEARDSLEY (1980) On the propagation of free topographic Rossby waves near continental margins. Part 2: Numerical model. *Journal of Physical Oceanography*, **10**, 1323–1339.

OVERLAND J. E. and R. W. PREISENDORFER (1982) A significance test for principal components applied to a cyclone climatology. *Monthly Weather Review*, **110**, 1–4.

PEDLOSKY J. (1979) *Geophysical fluid dynamics*. Springer-Verlag, New York, 624 pp.

PHILANDER G. (1978) Forced oceanic waves. *Reviews of Geophysics and Space Physics*, **16**, 15–46.

PREISENDORFER R. W., F. W. ZWIERS and T. P. BARNETT (1981) Foundations of principal component selection rules. SIO Ref. Ser. No. 81-4, May 1981, Scripps Institution of Oceanography, 192 pp.

RHINES P. B. (1970) Edge-, bottom- and Rossby waves in a rotating stratified fluid. *Geophysical Fluid Dynamics*, **1**, 273–302.

RODEN G. L. (1986) Thermohaline fronts and baroclinic flow in the Argentine Basin during the austral spring of 1984. *Journal of Geophysical Research*, **19**, 5075–5093.

THOMPSON R. O. R. Y. (1977) Observations of Rossby waves near Site D. *Progress in Oceanography*, **7**, 1–28.

THOMPSON R. O. R. Y. and J. R. LUYTEN (1976) Evidence for bottom-trapped topographic Rossby waves from single moorings. *Deep-Sea Research*, **23**, 629–635.

WALLACE J. and R. DICKINSON (1972) Empirical orthogonal representation of time series in the frequency domain. Part I: Theoretical considerations. *Journal of Applied Meteorology*, **11**, 887–900.

WATTS D. and H. T. ROSSBY (1977) Measuring dynamic heights with inverted echo sounders: Results from MODE. *Journal of Physical Oceanography*, **7**, 345–358.

WATTS D. and W. JOHNS (1982) Gulf Stream meanders: Observations on propagation and growth. *Journal of Geophysical Research*, **87**, 9567–9476.

WEBSTER F. (1961) A description of Gulf Stream meanders off Onslow Bay. *Deep-Sea Research*, **8**, 130–143.

WILLEBRAND J. (1977) Temporal and spatial scales of the wind field over the North Pacific and North Atlantic. *Journal of Physical Oceanography*, **8**, 1080–1094.